3. Geophysical Fluid Dynamics

Experimental study on the three dimensional spherical convections with the parameters of planetary atmospheres

Contact Person: Yoshi-Yuki Hayashi
Graduate School of Earth Environmental Science
Hokkaido University

Research Organization: Yoshi-Yuki Hayashi[1], Shin-ichi Takehiro[2]
Masaki Ishiwatari[3], Masahiro Hosaka[4]
Geophysical Fluid Dynamics Group,
Graduate School of Earth Environmental Science, Hokkaido University

Keywords: spherical convection, general circulation, planetary atmospheres, angular momentum, zonal mean flow, teleconnection patterns, SST anomaly, heating response

1. Background

The grand purpose of our study is to reveal the dynamical structures which underlie the general circulations of the planetary atmospheres. It is aimed to construct a theoretical framework which is useful in describing their circulation characteristics, as tried by Golitsyn[1] since 1960's ~. Our interest in due course is to recognize the atmosphere of the earth (or the climate of the earth) as one of the possible realizations in the physical parameter space observed in the solar system.

One of our procedures in revealing the possible underlying dynamics is to gather and classify atmospheric circulation patterns which might be observed under various values of planetary "external" conditions such as orbital parameters (amount and variation of the incoming solar flux), radius and rotation rate of the planet, radiation property of the atmosphere, and surface boundary setups. The sampling of the possible atmospheric circulations may be possible by numerical experiments by the use of the super computer powers.

Our search in circulation patterns is now performed for the following three major targets:

1. to reveal the possible circulations which might be realized with the earth's condition, but with strongly simplified surface and/or physical processes,
2. to reveal the possible circulations which might be realized with the values of solar flux and orbital parameters which are related to Mars, Earth and Venus,
3. to reveal the possible circulations which might be realized as convection of a spherical shell in general.

These are the targets being studied continuously from the preceding years.

The first target includes so called aqua-planet experiment, where all of the lower boundary surface is assumed to be covered by the ocean[2-4]. The aim is to answer the basic problem of the climate, that is, "where and how does it rain?". In the aqua-planet experiments performed so far, the focus has been placed on especially in searching for the idealistic precipitation distribution of the tropics. The experiment performed here is also in this category, however, the new feature is to find out the deformation of the precipitation distribution to a warm SST (sea surface temperature) anomaly placed in the tropics. The configuration is supposed to extract the effect of the warm SST region in the real Western Pacific on the general circulation patterns.

The second target is the three dimensional calculations of the so called runaway greenhouse effect. It has been argued, in relation to the evolution of the atmospheres of Venus, Earth and Mars, that there exists a limit of radiation which can be emitted from the top of the atmosphere with the ocean[5]. The interesting point is that the radiation limit predicted in the literature is not far from the value of the incoming solar flux of the present earth. It is about 300 W/m^2. The argument placed so far is presented by the use of one dimensional models. It is of interest to observe with three dimensional model to what extent the climate of present earth is stable to the variation of the solar constant. The present concern is to assess the calculation possibility of the evaporation or the freezing of the oceans.

The third target is to refine the dynamical framework of the rotating spherical convection theory, and also to acquire the description ability of the circulation patterns of the deep "atmospheres" as those of outer planets and the sun. The theory of convection in rotating spherical shells has been intensely considered by Busse and his colleagues[6]. The difficulty in their work is that the description utilized is too much mathematical, and hence it is not easy to acquire physical insight. Especially for the distribution of the angular momentum, there has not been presented any satisfactory mechanistic description.

Our activity this year has been focused on the parameter study of the aqua planet situation with vary-

[1] Present affiliation: Graduate School of Mathematical Science, University of Tokyo
[2] Present affiliation: Faculty of Science, Kyushu University
[3] Present affiliation: Graduate School of Earth Environmental Science, Hokkaido University
[4] Present affiliation: Numerical Prediction Division, Japan Meteorological Agency

ing vertical resolution of the model. As described below, we are now encountering a common difficult problem of numerical simulation of the atmospheres. We are finding that, for the purpose of simulating the runaway greenhouse state, it is necessary to calculate not only the troposphere but the middle atmosphere also. In order to extend the upper boundary of the model, however, we have to find a certain way to reconcile with the activity of gravity waves. We have to confess here that we could not have found a practical way to pass through the problem at the moment. Our model could not be integrated long enough to acquire the statistically thermal equilibrium state. Since the dynamical implementation of our model is basically the same as that of CCSR/NIES model, we are now collaborating with Dr. Sugata to beat this fundamental problem.

2. Experimental design

2.1 Model

The model utilized is basically the same as that used in [3]. It is the code originally produced by Dr. Numaguti of NIES, and is the version now archived and maintained by GFD-DENNOU CLUB. The model consists of the three dimensional hydrostatic system on a sphere with very crude physical processes. The dynamical part is represented by the pseudo spectral method with the triangular truncation at wavenumber 21 (T21) and 16 or 32 vertical levels. The horizontal resolution might be crucially small but still is able to represent baroclinic instability. As for the detail of the vertical resolution we will describe more in section 3.2.

The cumulus parameterizations are Kuo scheme or adjustment scheme or large scale condensation only. In this report, we will describe only the results with adjustment scheme. The vertical diffusion is represented by Yamada-Meller Level II scheme. The surface fluxes are evaluated by the usual bulk formula.

The surface is all covered by the ocean (aquaplanet). The value of SST is determined by the surface heat budget. The surface has no heat capacity, i.e., so called swamp ocean.

The radiation processes utilized is the exactly the same one as that of [5]. There is no scattering. Only the water vapor absorption of long wave radiation is included. Moreover, the absorption coefficient is constant (gray atmosphere). The sun is assumed to be at the equinox position. Hence the zonal mean incoming solar flux is symmetric around the equator.

2.2 Experimental Design

The first study performed this year is to determine the minimum but sufficient number of vertical levels needed for calculating radiation processes which can survive the situation realized even under the runaway greenhouse state. The vertical resolution used in the experiments of the preceding year (16 vertical levels) is lower than that of the one-dimensional model of [5] by an order of several tens (about 700 vertical levels). Since the purpose of the study last year was to assess the calculation possibility of the runaway state with the current general circulation model, it was reasonable to start with a low resolution version to shorten the integration time to reach the unexplored thermal parameter regime. We actually found that the model with 16 vertical levels show decreasing outgoing longwave radiation with time when the incoming solar flux is larger than the radiation limit expected by the one dimensional radiative convective equilibrium model. We expected that the model would be able to calculate the runaway greenhouse state. The results were stimulating but some of them were obviously beyond the limit of vertical resolution; the troposphere becomes too high for the 16 vertical level model to be resolved, and the atmosphere becomes quite thick in radiation so that the radiative transfer equation is not properly represented.

Now, in section 3.1 the detail of the determination of the vertical resolution is presented. It is based on the results of the one-dimensional radiative convective equilibrium calculations with various vertical resolution. It shows that we have to utilize at least 32 vertical levels for the three-dimensional calculation of the second study.

The second study of this year is to search the performance of the three-dimensional model with the above mentioned sufficient vertical resolution. We increased the vertical levels from 16 to 32. In section 3.2, the results for the case of the present earth condition, in which the solar constant is fixed to be 1380 W/m^2 are presented. The results of runaway case, in which the solar constant is fixed to be 1800 W/m^2, are shown in section 3.3. The difficulty we are now encountering is that the possibility of a long-term integration is not assured. A procedure which may make long-term integration possible is also described.

3. Some of the Results

3.1 Consideration on the vertical resolution

The one-dimensional equilibrium solutions are calculated by a model reduced from the three-dimensional model with various vertical grid levels. The results are compared with the solution calculated by [5]. The integration is performed from the surface $\sigma = 1$ to the level of $\sigma = 10^{-6}$, where σ is the ratio of the pressure to the surface pressure. The top level corresponds to about 100km altitude; around the mesopause in the case of the present earth. In the runaway greenhouse state, the tropopause may reaches up to such high altitudes.

We tested the following two types of vertical differentiation schemes for radiation transfer calculation. The first one is a scheme in which the whole atmosphere is divided into a thousand layers with equal height (hereinafter referred to as L1000-grid). The second one is a scheme in which the lower layers from the surface to the level of $\sigma = 0.05$ is divided into 16 levels with about equal thickness of σ and the upper layers above this level is divided into 16 layers with about equal geometric height (hereinafter referred to as L32-grid).

Figure 1 and Figure 2 show the relationship be-

tween ground temperature and outgoing longwave radiation at the top level (OLR) obtained using by L1000-grid and L32-grid, respectively. The results for various partial pressure p_{n0} of the non-condensable component at the surface, which is approximately the total pressure of the atmosphere when the water mixing ratio is small, are shown in the figures. The results obtained by using L1000-grid show good agreement with [5] if $p_{n0} < 10^7$ Pa. The results of L1000-grid and of L32-grid agree with each other when $P_{n0} < 10^5$ Pa. The difference of OLR for each results is 5 W/m^2 at most. When $P_{n0} < 10^5$ Pa, the vertical structure of the temperature and the vertical distribution of the radiation flux show quite good agreement between the calculations obtained by L32-grid and those by L1000-grid (Figures not shown).

For the sake of comparison, the result obtained by the model with 21 vertical levels is shown in Figure 3. Note that Figure 3 shows only the case of $p_{n0} = 10^5$ Pa. It is shown that, using such a low resolution model, the possible error in the radiation field becomes large and hence correct results of the runaway state may not be obtained.

Judging from the above results of one-dimensional radiative-convective models, L32-grid is sufficient for radiation calculation if $p_{n0} < 10^6$ Pa. The three-dimensional model should utilize the vertical resolution of this much.

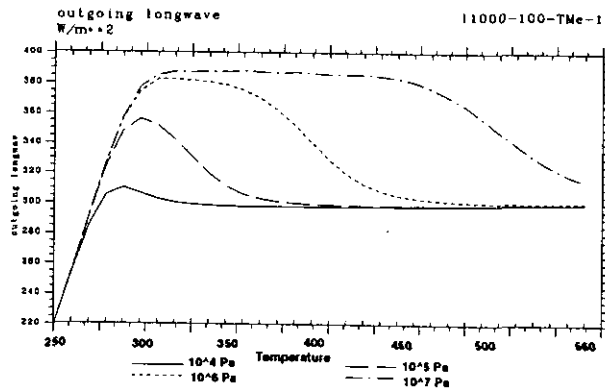

Figure 1. The relationship between OLR and T_s for the case of L1000-grid.

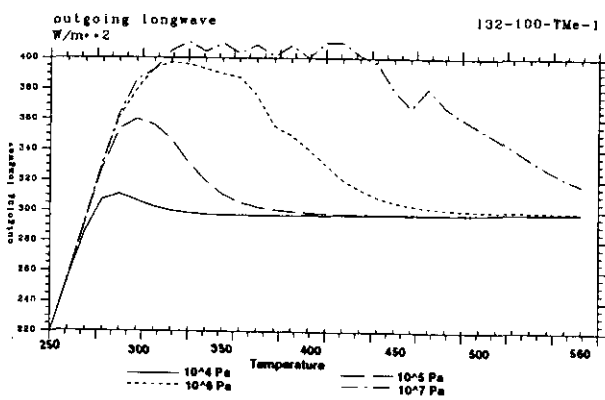

Figure 2. The relationship between OLR and T_s for the case of L32-grid.

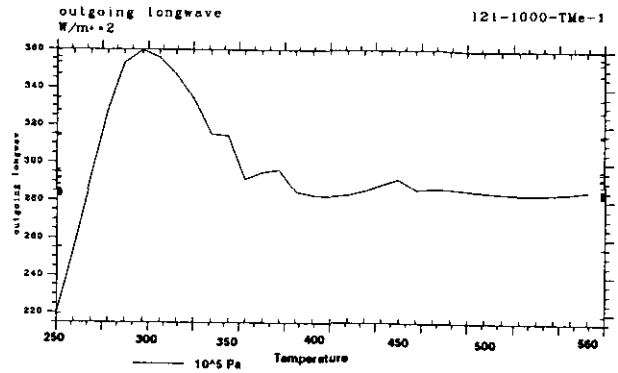

Figure 3. The relationship between OLR and T_s for the case of L21-grid.

3.2 Three-dimensional calculations of the earth condition with L32-grid model

In this section, the performance of the three-dimensional model with L32-grid is investigated. The solar constant is fixed to be 1380 W/m^2, The averaged solar flux over the glove is 345 W/m^2. This is, expect for the albedo effect, the value corresponding to the present earth condition.

First of all, experiments with a model whose scheme is the same as the one implemented in the model utilized in the study of the preceeding year. The vertical resolution is increased to have 32 levels enforced in the previous section. The result is that we cannot integrate more than 300 days. The reason for incapability of long-term integration seems to be the growth of vertically 2-grid noise. Unfortunately, we do not, at the moment, succeed in resolving the cause of the growth of 2-grid noise. We are now trying to find out the direct reason which causes this trouble.

Following the procedure utilized in GFDL SKYHI model ([7]), Rayleigh damping of horizontal wind and Newtonian cooling of temperature at the top level are introduced to remove the two grid noise. Now, this "improved" version of the model can be integrated for 1000 days, and still seems to be numerically stable. The results of the calculation are shown in Figure 4 and Figure 5. Figure 4 shows zonal mean temperature and Figure 5 shows zonal wind averaged from 950 day to 1000 day, respectively. The characteristic feature of the wind field is that the westerly wind appears in the upper layer of the tropics and the easterly wind appears in the midlatitude. Correspondingly, in the upper layer of the tropic,

the warm region exists.

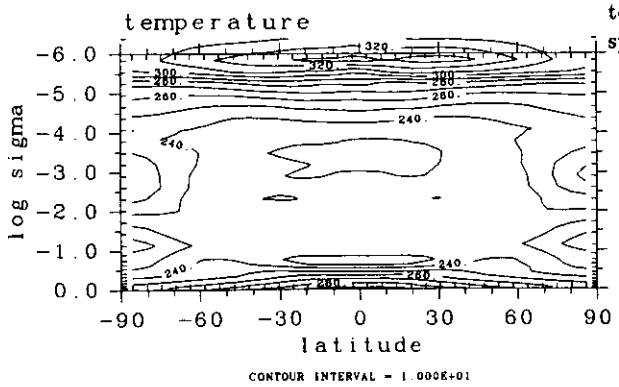

Figure 4 The zonal mean temperature field for the case of 1380 W/m^2.

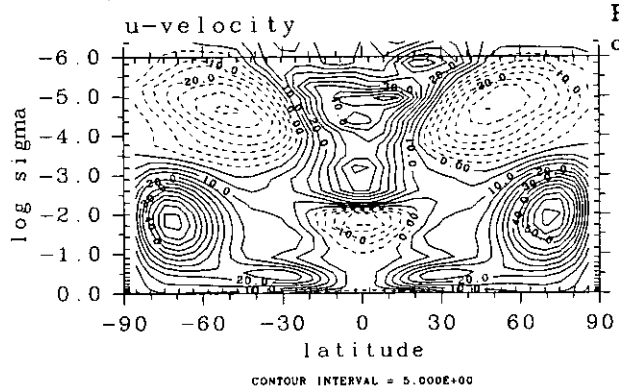

Figure 5 The zonal mean wind field for the case of 1380 W/m^2.

3.3 Three-dimensional calculation of the runaway condition with L32-grid model

When the solar constant is increased to 1800 W/m^2, the integration cannot be continued over 60 days even with the use of the model improved by introducing the Rayleigh damping and the Newtonian cooling at the top level. 1800 W/m^2 is the value of the solar constant with which the existence of the runway greenhouse was confirmed by the experiments of the previous year.

In order to enable the longer term integration, we have to introduce Rayleigh damping and Newtonian cooling in the upper 10 layers, and moreover we have to introduce a vertical smoothing filter in temperature and horizontal wind fields. The results of the altered model are shown in Figures 6 and 7. Figure 6 shows the zonal mean temperature field and Figure 7 shows the zonal wind field averaged from 2000 day to 2050 day, respectively. In the upper layer, both of temperature and zonal wind become almost homogeneous because of the effect of the vertical filter. The value of the global mean emission to outer space is about 350 W/m^2, which is well below the input solar flux, 450 W/m^2. The height of tropopause is now about $\sigma = 10^{-2}$ at the equator. The atmosphere is going to be in a runaway state.

Those results suggest that in order to continue a long-term integration, the two grid noise in the upper layer must be removed thoroughly when the model extending from the lower troposphere to the upper mesosphere is used.

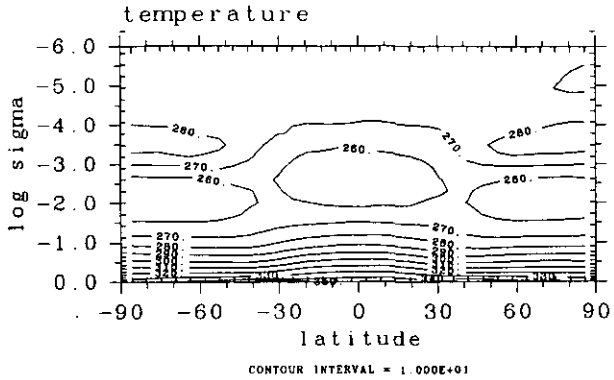

Figure 6 The zonal mean temperature field for the case of 1800 W/m^2.

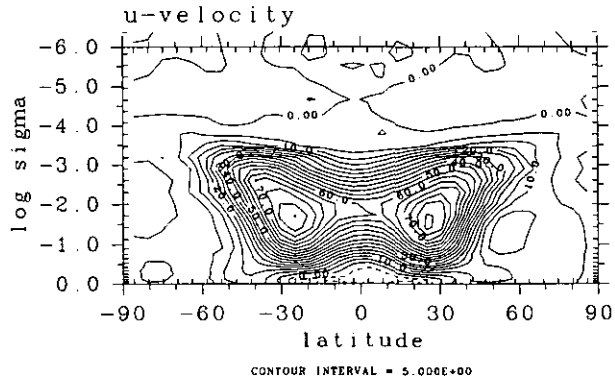

Figure 7 The zonal mean wind field for the case of 1800 W/m^2.

Acknowledgement

We wish to thank Drs. Mitsumoto, Numaguti, Sugata, Takayabu and other NIES staff members for providing us with this powerful computing facility. A number of suggestions and supports by Dr. Numaguti and Sugata on softwares, hardware usages, and sciences were indispensable to our research performance. Our software environment was provided from the resources of GFD DENNOU CLUB. GFD DENNOU CLUB is an independent group of scientists aiming at collecting basic software resources for research and education of geophysical fluid dynamics and related fields. Those resources include three dimensional spherical primitive system originally developed by Dr. Numaguti while he was at University of Tokyo. We also have to express our thanks to the staffs of TISN (Tokyo university International Science Network) in providing us with data connection between NIES and University of Tokyo.

References

1. G.S. Golitsyn, *ICARUS*, **13**, 1 (1970)
2. Y.-Y. Hayashi and A. Sumi, *J. Met. Soc. Japan*, **64**, 451 (1986)
3. A. Numaguti and Y.-Y. Hayashi, *J. Met. Soc. Japan*, **69**, 541 (1991)

4. A. Numaguti, *J. Atmos. Sci.*, **50**, 1874 (1993)

5. S. Nakajima, Y.-Y. Hayashi and Y. Abe, *J. Atmos. Sci.*, **49**, 2256 (1992)

6. K.-K. Zhang and F.H. Busse, *Geophys. Astrophys. Fluid Dynamics.*, **39**, 119 (1987)

7. E. Manzini and K. Hamilton, *J. Atmos. Sci.*, **50**, 2180 (1993)

Baroclinic instability of elliptic vortex in an imposed strain field

Contact Person TAKESHI MIYAZAKI,
Dept. of Mechanical and Control Engineering,
Univ. of Electro-Communications
Research Organization TAKESHI MIYAZAKI, HIDESHI HANAZAKI*
*Div. of Atmospheric Environment,
National Institute for Environmental Studies
Keywords Baroclinic instability, Elliptic vortex, Background Strain, Background vorticity, Resonant excitation of inertial wave

1. Introduction Concentrated vorticity region appears as a coherent structure in geophysical flows, where the fluid motions are subject to a strong influence both of the Coriolis force and the density inhomogeneity (stable stratification). Certain geophysical fluid motions are described by a quasi-geostrophic approximation fairly well and many investigations on vortex instability have been performed based on the quasigeostrophic, f-plane equations.

Miyazaki & Hanazaki (1994: MH) studied the linear baroclinic instability of Kirchhoff's elliptic vortex, i.e., a vortex patch with uniform vorticity ω_0 inside an ellipse whose major and minor semi-axes are a and b. It rotates solidly with a constant angular velocity $\Omega=\omega_0 ab/(a+b)^2$ if it is embedded in an irrotational fluid. According to Love's barotropic analysis (1893), it becomes unstable to disturbance with azimuthal wave number m=3, if the ratio a/b is greater than 3, whereas MH showed that Kirchhoff's ellipse is unstable to the baroclinic bending mode ($m=1$) and the baroclinic elliptical deformation ($m=2$) irrespective of the ratio a/b. The former instability ($m=1$) is caused by resonant interaction between the baroclinic bending waves and the barotropic elliptical deformation. The resonance occurs if the angular velocities of these modes (around the vortex axis) are identical.

We study the baroclinic instability of an elliptic vortex embedded in a strain field. Moore & Saffman (1971) obtained a series of steady solution representing a uniform (ω_0) elliptic vortex patch embedded in a uniform background straining field e with uniform vorticity 2γ ("the Moore-Saffman vortices"). They also performed 2D-stability analysis and showed that the ellipse in a pure strain is unstable to the m=2 mode (elliptical deformation) if the ratio a/b is greater than 2.9.

We formulate the eigenvalue problem for normal modes following MH. The perturbation streamfunctions, that obey the Helmholtz equation, are expanded in terms of the Mathieu functions. The eigenvalues are determined numerically after truncating the expansions at a finite order. The results of the stability analysis are demonstrated in Sec.3. It is shown that the baroclinic effects are important for weakly elongated ellipses, in the parameter range $-0.5 < \gamma < 0$. In Sec.4, we consider the physical mechanisms of instabilities in the limit of small ellipticity, where the twisting instability ($m=1$) is found to be excited by resonance between the baroclinic inertial (bending) wave and the imposed barotropic strain field (m=2 elliptical deformation).

2. Formulation The quasi-geostrophic equations of motion (conservation of the potential vorticity: e.g. Pedlosky 1979) on the f-plane are written in terms of a streamfunction ψ, as

$$[\frac{\partial}{\partial t}+\frac{\partial\psi}{\partial y}\frac{\partial}{\partial x}-\frac{\partial\psi}{\partial x}\frac{\partial}{\partial y}][\Delta+L_z]\psi=0. \qquad (1)$$

The streamfunction inside the Moore-Saffman elliptic vortex is given by,

$$\Psi_{in}=-\frac{1}{2}\Omega ab(\frac{x^2}{a^2}+\frac{y^2}{b^2}-1),\Omega=\frac{\omega_0 ab}{a^2+b^2}, \qquad (2a,b)$$

where the uniform (additional) vorticity in the interior of the ellipse is taken to be ω_0. The parameters a and b denote the major and minor semi-axese, respectively. The elliptic vortex is embedded in a uniform strain e with uniform background vor-ticity 2γ, i.e., the streamfunction

outside the vortex at the large distances from the vortex center is given as

$$\Psi_{out} \approx \frac{1}{2} e (x^2 - y^2) - \frac{1}{2} \gamma (x^2 + y^2) . \quad (3)$$

The elliptic-cylinder coordinates (ξ, η, z) are convenient in describing the geometry of the basic flow field:

$$x = \sqrt{a^2-b^2} \cosh\xi \cos\eta ,$$

$$y = \sqrt{a^2-b^2} \sinh\xi \sin\eta . \quad (4a,b)$$

In these coordinates, the boundary of the elliptic vortex is represented by

$$\xi = \xi_0 = \frac{1}{2} \log\left(\frac{a+b}{a-b}\right), \quad (5)$$

and the streamfunction outside the vortex is written as

$$\Psi_{out} = -\frac{ab}{2}(\omega_0 - 2\gamma)(\xi - \xi_0) + \frac{ec^2}{4}\cos2\eta(\cosh2\xi - \cosh2\xi_0 e^{2(\xi_0-\xi)}) \quad (6)$$

$$- \frac{\gamma c^2}{4}\{\cosh2\xi - \cosh2\xi_0 + \cos2\eta(1 - e^{2(\xi_0-\xi)})\}$$

We can not take all of these parameters (a, b, ω_0, e, γ) at will, if we confine our attention to a steady basic state. Steady solutions are permitted, only if the following condition is satisfied (Moore & Saffman 1971; see Kida 1981 for the general case):

$$e\frac{a+b}{a-b} - \gamma = \omega_0 \frac{ab}{a^2+b^2} . \quad (7)$$

In order to avoid the redundancy of the parameters, we assume that the vorticity inside the ellipse is greater than the background vorticity by unity ($\omega_0 = 1+2\gamma$).

We can introduce the normal-mode disturbances of the form

$$\Psi_{in,out} = \Psi_{in,out} + \varepsilon f(z) \hat{\psi}_{in,out}(\xi,\eta) e^{-i\omega t}, \quad (\varepsilon<<1), \quad (8)$$

where $f(z)$ denotes the eigenfunction of a Sturm-Liouville problem associated with the differential operator L_z (with appropriate boundary conditions). Thus, $f(z)$ corresponds to the eigenvalue λ, i.e.:

$$L_z f(z) = -\lambda^2 f(z). \quad (9)$$

The boundary of the vortex patch is assumed to deform as

$$\xi = \xi_0 + \varepsilon F(\eta) f(z) e^{-i\omega t}. \quad (10)$$

We consider the perturbations that do not introduce additional potential vorticity. Then, the disturbance streamfunctions (both inside and outside the ellipse) obey the Helmholtz equation:

$$\left[\frac{\partial^2}{\partial\xi^2} + \frac{\partial^2}{\partial\eta^2} - 2q(\cosh2\xi - \cos2\eta)\right]\hat{\psi}_{in,out} = 0,$$

$$q = \frac{1}{4}(a^2-b^2)\lambda^2. \quad (11)$$

At $O(\varepsilon)$, the kinematical boundary conditions are written, at $\xi=\xi_0$, as

$$i\omega h^2 F + \frac{\partial\hat{\psi}_{in}}{\partial\eta} - \Omega\frac{\partial}{\partial\eta}(h^2 F) = 0,$$

$$i\omega h^2 F + \frac{\partial\hat{\psi}_{out}}{\partial\eta} - \Omega\frac{\partial}{\partial\eta}(h^2 F) = 0, \quad (12a,b)$$

where h^2 denotes the metric factor:

$$h^2 = \frac{1}{2}(a^2-b^2)(\cosh2\xi - \cos2\eta). \quad (13)$$

The dynamical condition at $\xi=\xi_0$ is the continuity of tangential velocity, which is equivalent to the condition of pressure continuity :

$$\frac{\partial\hat{\psi}_{in}}{\partial\xi} - \frac{\partial\hat{\psi}_{out}}{\partial\xi} = h^2 F. \quad (14)$$

It is remarkable, here, that the eigenvalue problem is identical to that formulated for the Kirchhoff's rotating ellipse (MH) except for the difference of the value of Ω, which is now

$$\Omega = \frac{(1+2\gamma)\,ab}{a^2+b^2} \quad (15)$$

instead of

$$\Omega = \frac{ab}{(a+b)^2}$$

for Kirchhoff's ellipse of unit vorticity.

We calculate the eigenvalues numerically, based on a Galerkin method. The solutions of the Helmholtz equation are expanded in terms of the Mathieu functions. The 2π-periodic (in the variable η) odd modes are decoupled from the π-periodic even modes because of the symmetry of the basic flow field. Truncating the expansions at a finite order N, making the products of the boundary conditions with $ce_{2l-1}(\eta,-q)$ and $se_{2l-1}(\eta,-q)$ $(1 \le l \le N)$, and integrating from 0 to 2π, we obtain the following matrix-type relation:

$$(i\omega\mathbf{A} - \mathbf{B})\mathbf{v} = 0. \quad (16)$$

Here the matrix A is a $2N \times 2N$ diagonal matrix. The eigenvalues ω

and the eigenvectors of the matrix $-iA^{-1}B$ ($2N \times 2N$) are calculated numerically using the QR method. The truncation order $N = 20$ is sufficient to achieve the accuracy of four significant figures.

3. Results We will investigate the cases of pure strain ($\gamma=0$) and simple shear ($\gamma=e$, $\gamma=-e$), as in Moore & Saffman (1971). The parameter region $-0.5 < \gamma < 0$, where the baroclinic modes are more dangerous than the two-dimensional modes, is inquired in more detail.

3.1 pure strain ($\gamma=0$; $\Omega = ab/(a^2+b^2)$) We put the parameter Ω to be $ab/(a^2+b^2)$, in order to investigate the pure strain case $\gamma = 0$. We show, in Figs.1a and b, the calculated instability-growth rate as contours in λ-a/b plane for the case of pure strain. Since the odd (2π-periodic) and even (π-periodic) modes, are decoupled, we have depicted the result for the odd modes in Fig.1a and that for the even modes in Fig1b, separately.

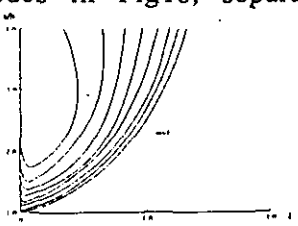

Fig. 1a

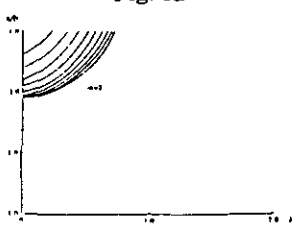

Fig. 1b

The horizontal axis is the vertical wavenumber λ (the eigenvalue of L_z) and the vertical axis is the ratio a/b. The contour interval is 0.02. Using these figures, we can judge whether an ellipse of a given aspect ratio a/b in a strain field e is stable or unstable, if the spectrum $\{\lambda_n\}$ of the Sturm-Liouville problem (9) is known.

The odd-instabilities are characterized by the azimuthal wavenumber m=1, in the parameter region shown (the m=3 instability modes are presented for $a/b > 4.54$, $\lambda = 0$). The two-dimensional modes ($\lambda = 0$) are unstable as has been commented above. The two-dimensional m=1 disturbance corresponds to a drifting motion of the center of vortex patch without change of ellipse-form. It is noted that the baroclinic mode with long wavelength is, slightly, more unstable. As the wavenumber is increased further, the growth rate decreases, indicating that the bending instability is, essentially, of long wave nature. These observations should be contrasted with the asymptotic estimate of Moore-Saffman (1971), which tells the three-dimensionality of bending disturbances, that obey the three-dimensional Euler equations, suppresses the m=1 instability monotonically (see, also, Robinson & Saffman (1984)).

The even modes, shown in Fig.1b, are the m=2 (elliptical deformation) modes. The fastest growing mode is the two-dimensional one (it destabilizes for a/b larger than about 2.89, reproducing the result of Moore-Saffman) and the growth rate decreases monotonically as λ is increased. We conclude from these observations that the baroclinic effects are not so destructive for stationary ellipses in a pure strain field.

3.2 simple shear ($\gamma = e, -e$; $\Omega = a/(a+b), \ b/(a+b)$) The major axis of the stationary ellipse in a simple shear $\gamma = e > 0$ is parallel to streamlines at infinity. The value of Ω is changed to a/(a+b). Moore & Saffman showed these ellipses are stable for any small perturbations. We cannot find out any unstable baroclinic modes in this case ($\gamma = e > 0$), too. These vortices seem to be stable both barotropically and baroclinically. The fact may have some relevance to the longevity of Jovian Great Red Spot.

In contrast, the steady ellipse, whose major axis is perpendicular to the shear flow ($\gamma = -e < 0$; $\Omega = b/(a+b)$), is unstable against the m=2 barotropic disturbances if $a/b > 2.41$, whereas it is stable to any odd barotropic modes. The baroclinic effects on the odd modes are substantial in this case. Figures 2a (odd modes) and b (even modes) depict the contours of constant growth-rate in the λ-a/b plane. As for even modes, only the m=2 modes appear in the parameter region described in Fig.2b.

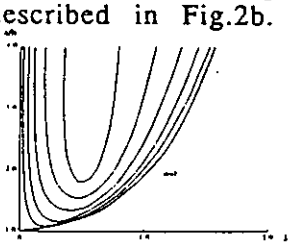

Fig. 2a

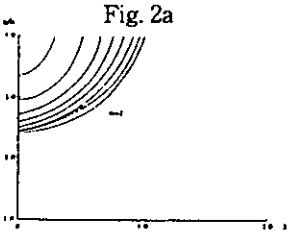

Fig. 2b

The two dimensional modes are the most dangerous modes and the baroclinicity of disturbances suppresses the instability growth rate. It is remarkable, however, that any ellipse becomes unstable to the m=1 baroclinic mode in Fig.2a, irrespective of the value of a/b. The growth rate increases and the unstable λ-range becomes wider as the ratio a/b increases. The baroclinic modes are more unstable than two-dimensional modes for ellipses whose aspect ratio is less than about 2.75. It suggests that some physical mechanisms are intesifying baroclinic instabilities in the parameter region $\gamma < 0$.

3.3 the parameter region -0.5 < γ < 0 In order to investigate the characteristics of baroclinic instabilities in more detail, let us fix the parameter γ to certain negative values in the range -0.5 < γ < 0, i.e., -0.15 and -0.35.

Figures 3a and b show the instability growth rate for γ = -0.15.

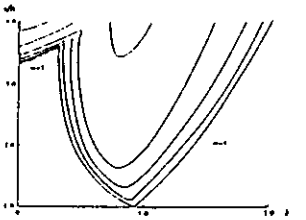

Fig. 3a

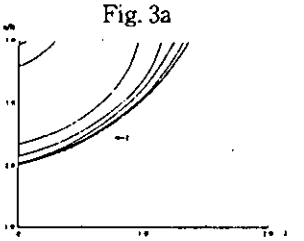

Fig. 3b

There are found, in Fig.3a, two instability branches of different character, of which the longer modes are the m=3 mode and the shorter modes are the m=1 (bending) mode. The m=3 instability (of barotropic origin) is suppressed monotonically as λ increases, whereas the m=1 short wave instability attains its maximum growth rate at about λ = 0.8. Its origin is, definitely, baroclinic, for the m=1 instability branch reaches the λ-axis at λ_C = 0.938. Any ellipse, irrespective of the value of a/b, becomes unstable to this mode if the critical eigenvalue λ_C belongs to the spectrum $\{\lambda_n\}$ of the Sturm-Liouville problem (9). We depict, in Fig.3c, the streamfunction of disturbance (a/b=2.0, λ=0.78) as contours in the x-y plane. It is clearly seen that the mode shows an azimuthal variation of m=1. The disturbance streamfunction resembles that of Fig.2b in MH. The baloclinic bending modes grow faster than the barotropic mode when a/b is less than about 3.8.

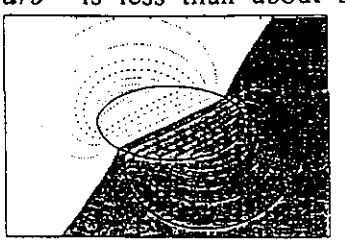

Fig. 3c

The even mode in Fig.3b are the m=2 mode. They are, again, suppressed as λ increases for $a/b <$ 2.8 but the maximum growth rate is attained at finite (nonzero) value of λ for $a/b > 2.8$. We notice, comparing Fig.3b with Fig.1b, that the instability band moves downward as γ decreases, which suggests that the character of the even (m=2) modes is changing from baratropic to baroclinic nature, too, as γ is decreased.

These trends become more evident for the case of $\gamma = -0.35$. We see, in Fig.4a, two banches touch the λ - axis, of which the shorter one (λ_C =3.195) is the m=1 mode and the longer (λ_C =1.39) is the m=3 mode. The contour interval is changed from 0.02 to 0.005, since the instability growth rate becomes smaller. The stream-functions of disturbance of the two modes are figured in Figs.4c (a/b=2.0, λ=2.85) and d (a/b=2.0, λ=1.74), respectively. Similarly, the band of the m=2 mode reachs the λ- axis at about λ = 2.53 (Fig.4b). The disturbance stream-function of the m=2 mode is shown in Fig.4e. There seems to be a qualitative difference between it and Fig.8b in MH. It may be because of the difference of character of the m=2 mode. Here, it is a baroclinic mode, whereas the m=2 mode in MH is essentially of barotropic nature. Any ellipse may, possibly, be unstable to these three baroclinic instabilites, even if it is baro-tropically stable.

As γ tends to -0.5 from above, more and more higher modes become barocilinically unstable, although their growth rate decreases in the same limit. In short, ellipses that are slightly elongated are apt to destabilized by baroclinic instabilities in the parameter region $-0.5 < \gamma < 0$. The physical explanation of these results are attempted in the next section.

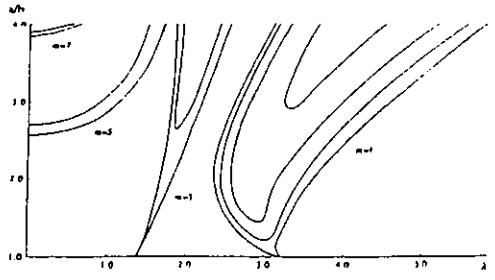

Fig. 4a

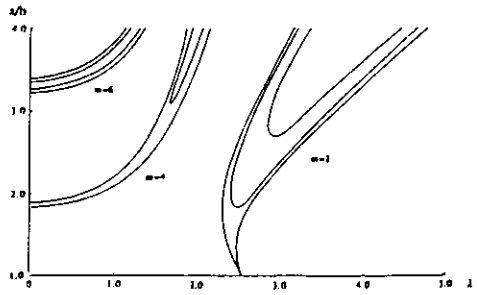

Fig. 4b

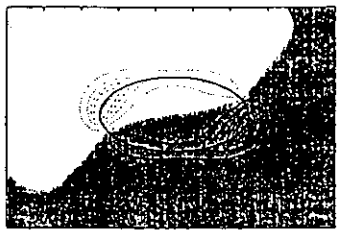

Fig. 4c

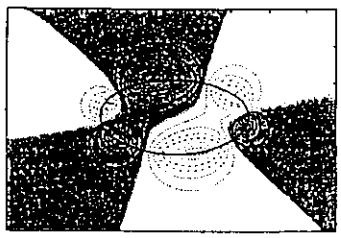

Fig. 4d

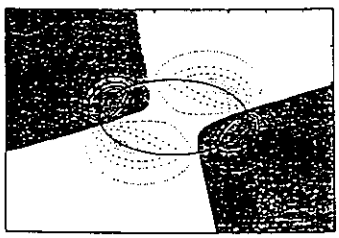

Fig. 4e

4. Discussions This section attempts to give a clear physical interpretation of baroclinic instabilies, i.e., the m=1 (bending wave), the m=2 (elliptical deformation) and higher modes (m>2), observed in the parameter region $-0.5 < \gamma < 0$, by investigating the nature of inertial waves in the limit of small ellipticity. The dispersion relation of inertial waves on Rankine's combined vortex is given by

$$\omega(m, \lambda) = m\,[\gamma + \frac{1}{2} - I_m(\lambda)K_m(\lambda)]. \qquad (17)$$

Figures 5a,b show the dispersion relations of several modes (m=1, 2, 3,---), where the horizontal and vertical axes are λ and $\omega'=\omega/m-\gamma$, respectively. The broken lines are the lines representing $\omega'=0.15$ and 0.35. We notice the meaning of the critical wave numbers λ_C appeared in the previous section. They are the zeros of the dispersion relations (17). The bending baroclinic (m=1) wave of $\lambda_C=0.938$ for $\gamma=-0.15$, for example, is a stationary wave, which is amplified if a stationary strain field e is superimposed, causing the instability. Three (m=1, 2 and 3) modes are excited through similar resonance for $\gamma=-0.35$. This is the physical mechanism of the baroclinic instabilities. As γ tends to -0.5 from above, the curve of dispersion relation (of higher modes) crosses the λ-axis, leading to occurrence of higher instabilities, successively. Thus, we have seen that the resonant interaction between the inertial waves and the imposed strain field does play a key role in the baroclinic instability.

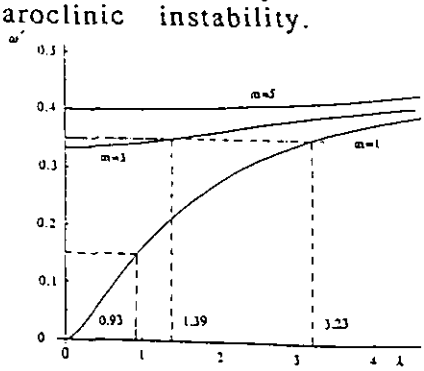

Fig. 5a

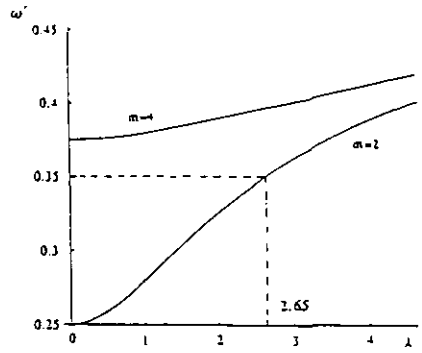

Fig. 5b

5. References

KIDA, S. 1981 *J. Phys. Soc. Japan* **50**, 3517-3520.

LOVE, A.E.H. 1893 *Proc. London Math. Soc.* **25**, 18-42.

MIYAZAKI, T. & HANAZAKI, H. 1994 *J. Fluid Mech.* **261**, 253-271.

MOORE, D.W. & SAFFMAN, P.G. 1971 *Aircraft Wake Turbulence* (ed. Olsen, Goldburg & Rogers), pp. 399-354. Plenum.

PEDLOSKY, J. 1979 *Geophysical Fluid Dynamics*. Springer, 624 pp.

ROBINSON, A.C. & SAFFMAN, P.G. 1984 *J. Fluid Mech.* **142**, 451-466.